



OPEN Spatiotemporal distribution prediction of the relict and endangered plant *Tetraena mongolica* in inner Mongolia, China under climate change

Jingxia Guo^{1,2}, Mingxu Zhang⁴, Yaqiong Bi³, Zezuan Zhao¹, Ran Wang¹ & Minhui Li^{1,2,3}✉

Climate change significantly affects the distribution of plant species, particularly that of relict plants. *Tetraena mongolica* Maxim. is a first-class endangered relict plant in China, primarily found in Inner Mongolia. This study explored the impact of multiple factors on its potential distribution under climate change. Considering a comprehensive set of 42 potential influencing variables, including climate, soil, net primary productivity (NPP), human activities, and topography, 29 variables were selected. The maximum entropy (MaxEnt) model was used to construct separate climate and soil niche models, and an “overlay function” was employed to construct a dual-suitability model. By establishing five different scenarios, we analyzed the effects of climate, human activities, and NPP on *T. mongolica* distribution. The results showed that climate is the most significant factor, soil constraints limit its distribution, and human activities reduce its suitable habitats. Although the direct influence of NPP is limited, it may indirectly affect *T. mongolica* distribution by improving habitat conditions. Future climate change is expected to sharply reduce suitable habitat areas, with the center of distribution migrating eastward. The study’s findings imply that climate change, human activities, and soil conditions significantly impact the distribution and survival of the endangered plant *T. mongolica*, necessitating comprehensive conservation measures to mitigate habitat loss and ensure its preservation.

Keywords Climate, Endangered, Human, Niche modeling, NPP, Relict, *Tetraena mongolica*

Climate change has profoundly impacted the natural distribution of species, biodiversity, and ecosystem sustainability¹. Rapid societal development has led to increased greenhouse gas emissions, resulting in more frequent extreme climate events, which further intensify the impact of climate change on ecosystems². Studies reveal that climate change is a major cause of biodiversity loss, habitat fragmentation, and changes in species spatial patterns^{3–5} and may increase the extinction risk for endangered species⁶. Therefore, a detailed understanding of the distribution and potential habitats of endangered species is essential to developing conservation plans and management strategies⁷. Studying the distribution of endangered species helps identify their primary growth locations and potential habitats, thus providing a foundation for targeted conservation measures^{8,9}. Additionally, understanding the impact of climate change on the distribution of endangered species helps predict further habitat changes, which is crucial for their conservation and sustainable use^{10,11}. Research on endangered species distribution and habitats can help elucidate how climate change affects their living environments, offering scientific support for future conservation and management efforts.

Tetraena mongolica Maxim. (*T. mongolica*), a highly drought-resistant deciduous shrub in the family Zygophyllaceae, belongs to the monotypic subfamily Tetraenoideae, which contains only this single genus and species¹². From ancient Mediterranean flora, approximately 140 mya, *T. mongolica* is a relict species classified as a first-class endangered plant in China¹³. Known as a “living fossil” and the “giant panda” of the plant world¹⁴, it has witnessed millions of years of climate, geomorphology, and soil change, making it an ideal subject for species distribution and biodiversity studies¹⁵. Although *T. mongolica* is globally distributed, most records are

¹Baotou Medical College, Baotou, Inner Mongolia, China. ²Inner Mongolia Key Laboratory of Characteristic Geoherbs Resources Protection and Utilization, Baotou, Inner Mongolia, China. ³Inner Mongolia Traditional Chinese & Mongolian Medical Research Institute, Hohhot, Inner Mongolia, China. ⁴State Key Laboratory for Quality Ensurance and Sustainable Use of Dao-di Herbs, Beijing, China. ✉email: prof_liminhui@yeah.net

concentrated in the Inner Mongolia, Ningxia, and Xinjiang regions of China, particularly in Inner Mongolia (Fig. 1). In other countries, such as Russia and Ukraine, it is sporadically found¹⁶. Despite multiple distribution records, information on the population size and range of *T. mongolica* is relatively limited. With its unique climate and topography, Inner Mongolia has become the primary distribution area for *T. mongolica*. This plant exhibits exceptional drought resistance, enabling its survival and reproduction in arid and harsh environments. Its deep root system effectively absorbs soil moisture, aiding the maintenance of the local ecosystem water balance^{17,18}. As the foundation for plant growth, soil provides the necessary water and nutrients, and the interaction between plant roots and soil nutrients determines plant distribution^{19,20}. As a key member of desert communities, *T. mongolica* prevents soil erosion, slows desertification, and maintains soil fertility and stability²¹. *T. mongolica* is indispensable for maintaining the stability of Inner Mongolia's ecosystems and protecting its ecological environment. However, in recent years, intensified global climate change and excessive exploitation of biological resources by human activities have altered species patterns, severely threatening *T. mongolica*'s habitat, leading to a sharp population decline and posing an extinction risk^{22,23}. Therefore, understanding its geographic distribution patterns and protecting its ecological habitats is critical.

Grasslands, one of the primary terrestrial ecosystems on Earth, are important for maintaining the natural environment and promoting sustainable socioeconomic development^{24–26}. China's grassland area covers 3.93 million km², accounting for 40% of the country's total land area. Over 20% of these grasslands are in Inner Mongolia, representing 13% of the world's grassland area^{27,28}. However, recent severe grassland degradation in Inner Mongolia has led to desertification and significant carbon sink loss²⁹. *T. mongolica*, a key species in grassland-desert communities, is crucial to the Inner Mongolian grassland ecosystem, aiding in windbreaks, sand fixation, soil conservation, and maintaining desert and grassland ecosystem stability. Net primary production (NPP) is an important ecological indicator that reflects the total energy plants obtain from the environment through photosynthesis for growth, development, and reproduction and is a crucial component of global carbon absorption³⁰. NPP measures plant growth capacity and is crucial for assessing ecosystem health and functional status³¹, providing a valuable reference for evaluating the ecological environment and sustainable development of ecosystems. Studying the influence of NPP on the geographic distribution of *T. mongolica* helps in understanding the mechanism by which vegetation distribution patterns form in grassland-desert areas, providing a scientific basis for grassland ecosystem protection and management. Previous studies on the potential geographic distribution of this species and its response to climate change^{14,32}, have made significant attempts to address this issue. However, further analysis of the results is required due to the different research objectives, environmental variables, and species distribution model constructions.

Ecological niche models (ENMs), also known as species distribution models (SDMs), are widely used to predict potential distribution areas for species. They use various algorithms to combine environmental variables with geographic data to simulate the ecological niches of species and project their potential distribution across the geographic landscape³³. Quantifying the ecological niches of species aids in understanding their geographic distribution changes, assessing their vulnerability to climate change and ecological adaptation, and promoting biodiversity maintenance³⁴. With advancements in computer technology and statistical science, different types of ENMs have emerged, including generalized linear models (GLM)³⁵, generalized additive models (GAM)³⁶, random forest (RF)³⁷, and maximum entropy (MaxEnt)³⁸. Among these, the MaxEnt model is widely used because it requires only presence data, can handle small sample sizes^{39–41}, and accommodates continuous or categorical data as inputs for environmental variables⁴².

Therefore, to better protect *T. mongolica*, this study comprehensively explores multiple driving factors to fully understand their impacts on the potential geographic distribution of *T. mongolica* under climate change, aiming to develop more effective conservation measures. To this end, this study employs the MaxEnt model to establish a climate niche model, considering multiple factors, including climate, NPP, human activities, and topography. This model simulates the distributional changes in the relict plant *T. mongolica* in Inner Mongolia, China, driven by multiple factors under climate change. Furthermore, the MaxEnt model will be used to analyze and establish a soil requirement niche model that will be combined with the climate niche model to construct a dual-suitability model to predict the potential geographic distribution of *T. mongolica* in Inner Mongolia. By comprehensively considering the influencing factors, this study aims to fully understand the impacts of multi-factor drivers on the potential distribution of *T. mongolica* under climate change conditions, providing an important reference for further research and conservation efforts.



Fig. 1. The habitat of *T. mongolica* in Inner Mongolia, China. (a) Single *T. mongolica*; (b) Flowering of *T. mongolica*; (c) Landscape of *T. mongolica*.

Results

Evaluation of model prediction results

The MaxEnt model was used to obtain the area under the curve (AUC) values for each model (Fig. 2). All AUC values were > 0.9 , indicating good model performance and high accuracy.

Key predictive variables

The MaxEnt model predictions indicated that under the climate change scenarios (Model A), the key climatic variables influencing the potential geographic distribution of *T. mongolica* included the minimum temperature of the coldest month (bio6), precipitation of the wettest month (bio13), and precipitation of driest month (bio14).

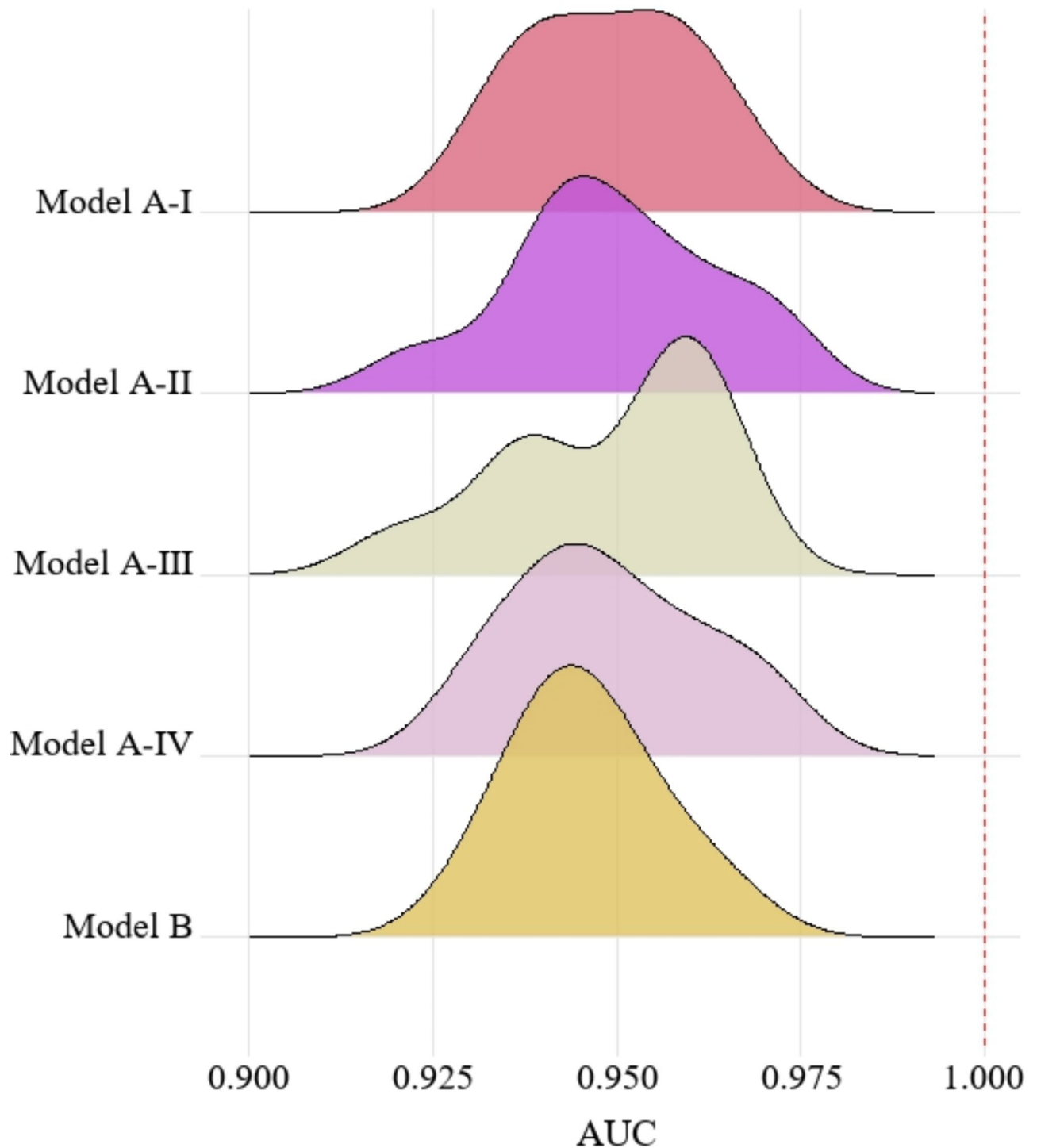


Fig. 2. The AUC values of different models.

In the four scenarios (I–IV) in Model A, these three key climatic variables contributed > 10% with cumulative contributions of 73.3, 70.2, 61.4, and 58%, respectively, suggesting that temperature and precipitation are key climatic variables affecting *T. mongolica*'s distribution (Fig. 3). The cumulative contribution rates of scenarios I–IV are 85.7, 85.1, 85.2, and 85.5%, respectively, with the common major variables being bio6, bio13, bio14, slope, bio3, bio8, bio15, aspect, bio5, and elevation (Table S3, Table S4).

Additionally, based on Scenario I, scenarios II, III, and IV incorporate NPP, human activities, and NPP and human activities, respectively. When comparing scenarios II, III, and IV to Scenario I, introducing different predictive variables led to varying changes in the key variables. In Scenario II, bio6 decreases by 11.7%, bio13 increases by 9%, and bio14 decreases by 0.4%. In Scenario III, bio6 decreases by 6.9%, bio13 by 0.8%, and bio14 by 4.2%. In Scenario IV, bio6 decreases by 11.2%, bio13 increases by 0.3%, and bio14 decreases by 4.4%. Notably, in Scenario III, the changes in the key variables were more pronounced, with human activities contributing 13.6 and 15.3% in scenarios III and IV, respectively. This suggests that human activities significantly impact the distribution of *T. mongolica*, whereas NPP contributes less in scenarios II and IV, and its influence on key factors is relatively insignificant compared with that of human activities.

Potential distribution of *T. Mongolica*'s dual suitability under current and future climate change conditions

Figure 4 shows the dual potential habitat suitability distribution of *T. mongolica* under four current climate scenarios. Suitable areas are primarily located in southwestern Inner Mongolia, particularly in regions such as Wuhai, western Ordos, southern Bayannur, and eastern Alxa League, with highly suitable areas distributed in Wuhai and western Ordos. Under the future climate scenarios, the potential habitat distribution of *T. mongolica* (Fig. 5), compared with that in the current climate scenario, showed that while some areas, such as Wuhai and western Ordos, may remain suitable, the overall distribution is expected to significantly fragment and the suitable habitat area is anticipated to decrease significantly.

Predictions of *T. Mongolica*'s potential habitat distribution under current climate conditions across four models

Figure 6 shows the dual habitat suitability distribution classification of *T. mongolica* under the current climate scenario using the four models and area predictions (Table 1). Under the scenario influenced only by climatic factors (Model A-I-B), the highly suitable habitat area was 0.2821×10^4 km², mainly in the northern and southern parts of Haibowan District, northern Hainan District, and scattered in Wuda District of Wuhai City; western Hangjin Banner, and northwestern Etoke Banner in Ordos City; and eastern Alxa Left Banner in the Alxa League. The moderately suitable habitat area was 0.2951×10^4 km², primarily distributed in the western part of Hainan District, northwestern Hangjin Banner, northwestern Etoke Banner, eastern Alxa Left Banner, and scattered in Dengkou, Hangjinhou Banner, Linhe, and Urad Middle Banner in Bayannur City. The low-suitability habitat area was 0.5739×10^4 km², sporadically distributed in the eastern part of Alxa Left Banner and scattered in Hangjin Banner, Dengkou, and Linhe. Suitable areas accounted for 0.9723% of the entire Inner Mongolian region, indicating that the habitat of *T. mongolica* is minimal. After incorporating NPP (Model A-II-B), although the distribution area did not change significantly, it varied. The highly suitable habitat area decreased to 0.0159×10^4 km², the moderately suitable habitat area slightly decreased to 0.2881×10^4 km²,

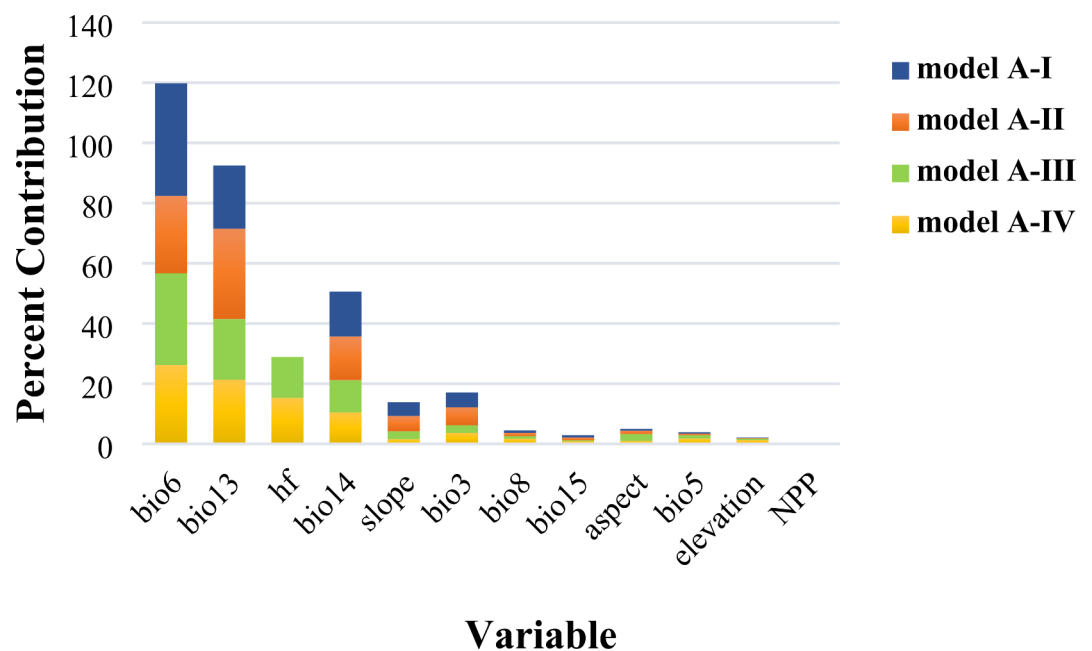


Fig. 3. The contribution rates of major variables in different models.

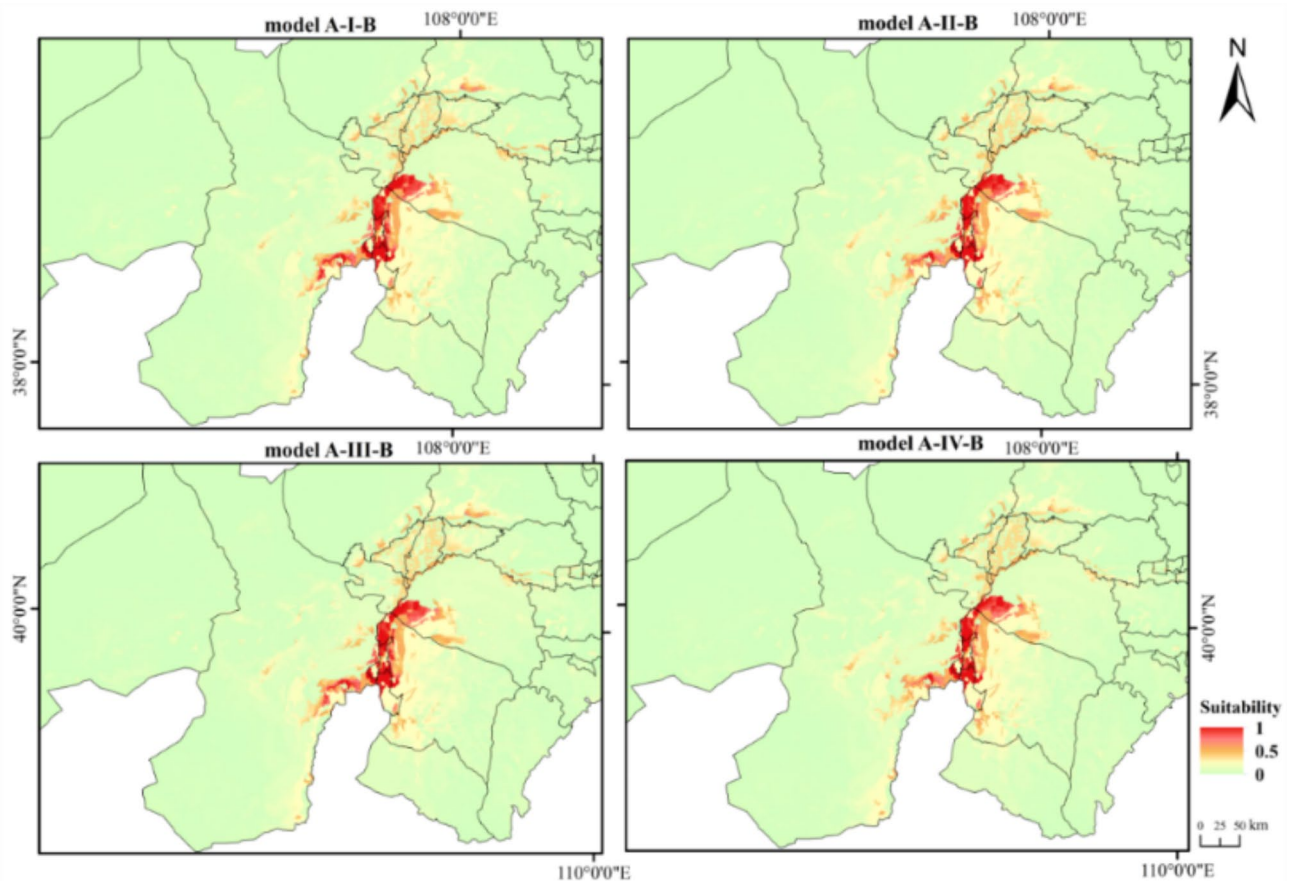


Fig. 4. Dual potential habitat suitability distribution of *T. mongolica* under current climate scenarios. Maps created in ArcGIS 10.8 (<https://www.esri.com/zh-cn/arcgis/products/arcgis-desktop/resources>).

and the low-suitability habitat area increased to 0.5878×10^4 km². Compared with Model A-I-B, the overall suitable habitat area decreased by 0.7819%. After adding human activities (Model A-III-B), the distribution area was unchanged but varied. The highly, moderately, and lowly suitable habitat areas decreased to 0.2716×10^4 , 0.2768×10^4 , and 0.5661×10^4 km², respectively. Compared with Model A-I-B, the overall suitable habitat area decreased by 3.1796%. When NPP and human activities were added (Model A-IV-B), the distribution area remained unchanged; however, it varied to different extents. The highly and moderately suitable habitat areas decreased to 0.2575×10^4 and 0.2659×10^4 km², respectively, and the lowly suitable habitat area increased to 0.6078×10^4 km². Compared with Model A-I-B, the suitable habitat area decreased by 1.7288%. Overall, human activities most significantly affect the habitat distribution of *T. mongolica*, with some mitigation by NPP based on the results from Model A-IV-B.

Changes in the potential distribution pattern of *T. mongolica* under future climate scenarios

Under future climate scenarios, the predicted suitable habitats of *T. mongolica* are primarily distributed in Etuoke Banner and Hangjin Banner in Ordos City; Wuda District, Hainan District, Haibowan District in Wuhai City; sporadically in Alxa Left Banner in the eastern part of the Alxa League, as well as in Dengkou, Urad Rear Banner, and Linhe in the southern regions of the Bayannur League. The highly suitable area decreased remarkably and became increasingly fragmented (Fig. 7). The most significant increase in suitable area under different climate scenarios occurred under SSP585 (2041–2060), covering 1.2297% of the entire region and representing the largest suitable area. However, at this stage, most suitable areas had low suitability, with highly suitable areas comprising only 5.68%. In comparison, under Model A-I-B, highly suitable areas comprised 24.51% of the suitable areas. The most significant decrease in the suitable area was observed under SSP126 (2041–2060), where the suitable area covered 0.82% of the overall region, representing the smallest suitable area (Table 2). Analysis of the percentage of suitable habitat areas indicated that, over time, the suitable habitat for *T. mongolica* under SSP126 and SSP245 initially decreased and then increased, whereas that under SSP585 showed the opposite trend, with highly suitable areas increasing. This suggests that the suitable habitat area of *T. mongolica* changes under different CO₂ emission levels and tends to stabilize; however, the overall suitable area decreases compared with the current area.

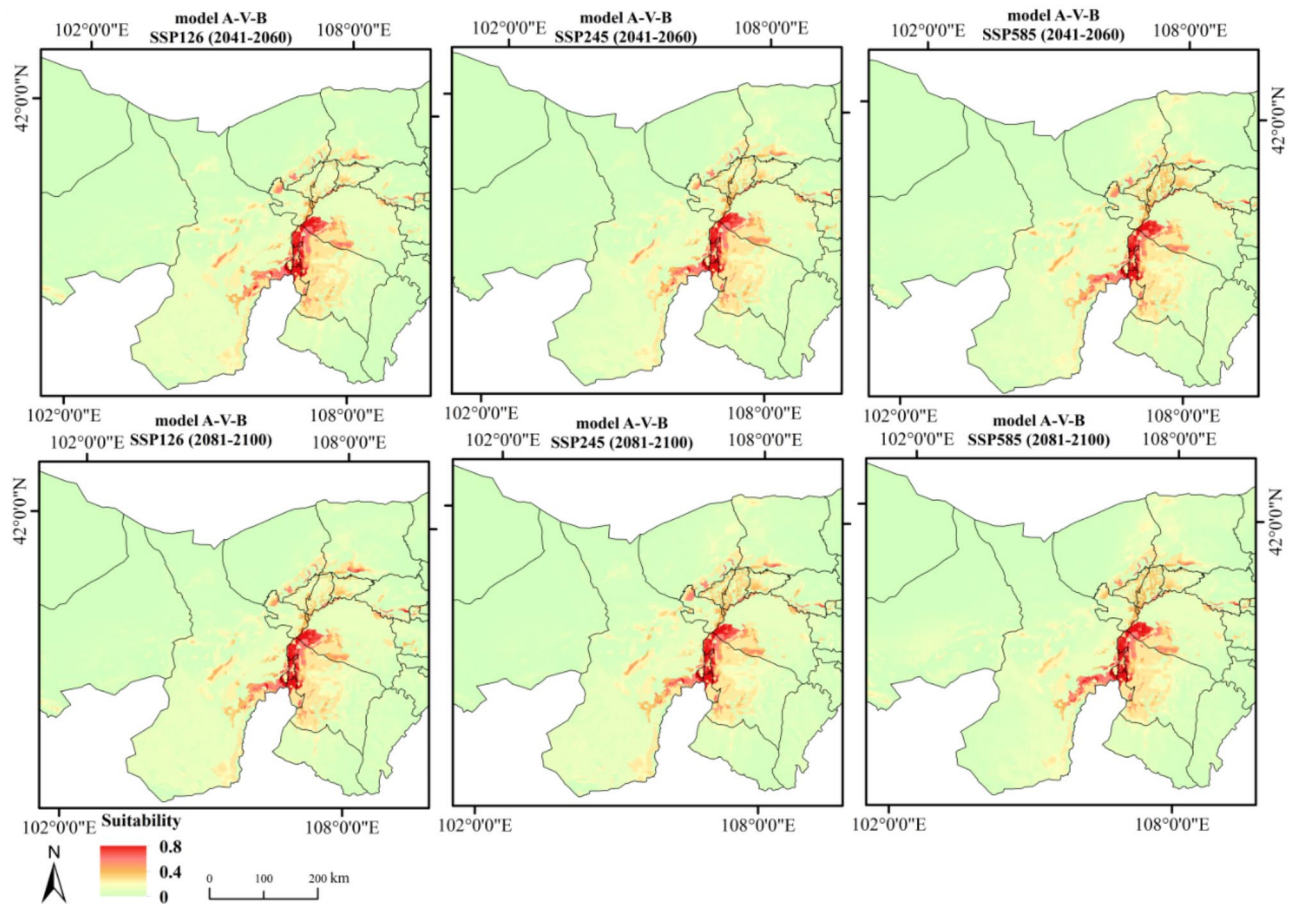


Fig. 5. Dual potential habitat suitability projection for *T.* under future climate scenarios. Maps created in ArcGIS 10.8 (<https://www.esri.com/zh-cn/arcgis/products/arcgis-desktop/resources>).

Temporal and spatial changes in ecological niches

Using the “Distribution Changes Between Binary SDMs” tool, the distribution results of *T. mongolica* at different times under the same Shared Socioeconomic Pathways (SSP) were analyzed. The results indicated that under the three different SSPs, the changes in *T. mongolica*'s expansion area were in the order of highly < moderately < lowly suitable habitats. The contraction area changes were in the order of high- < low- < moderate- suitability habitats. Unchanged areas were in the order of highly < moderately < lowly suitable habitats. Furthermore, with increasing CO₂ concentrations, the expansion areas of high-, medium-, and low-suitability habitats generally displayed an initially decreasing and then increasing trend, while the contraction area initially increased and then decreased (Table 3). The regions where the suitable habitat for *T. mongolica* initially expanded and then contracted were mainly in the Alxa Left Banner and the southwestern region of the Bayannur League. The regions where suitable habitats remained relatively unchanged were mainly Wuda District, Haibowan District, Hainan District, Etuoke Banner, and Hangjin Banner. Additionally, the habitat area of *T. mongolica* changed with varying CO₂ concentrations (Fig. 8). Under the SSP585 (2041–2060) scenario, the expansion area was highest at 0.8012×10^4 km², primarily distributed in Alxa Left Banner, Dengkou, and Linhe. Under the SSP245 (2041–2060) scenario, the expansion area was lowest at 0.4743×10^4 km², mainly in the Alxa Left and Hangjin banners. Under the SSP126 (2081–2100) scenario, the contraction area was highest at 0.7672×10^4 km², primarily in the southwestern regions of Bayannur, including Hangjin Rear Banner, Linhe, and Dengkou. Under the SSP585 (2041–2060) scenario, the contraction area was lowest at 0.4549×10^4 km², mainly distributed in the Alxa Left Banner and Linhe. Under the SSP585 (2041–2060) scenario, the unchanged area was highest, at 0.8567×10^4 km², mainly distributed in the Wuda District, Haibowan, Hainan District, Etuoke Banner, Hangjin Banner, Linhe, and parts of the eastern Alxa Left Banner. Under the SSP126 (2081–2100) scenario, the unchanged area was lowest, at 0.5447×10^4 km², primarily concentrated in the Wuda District, Haibowan, Hainan District, Etuoke Banner, Hangjin Banner, and parts of eastern Alxa Left Banner (Fig. 8; Table 3).

Using the “Centroid Changes (Lines)” tool in “SDMtoolbox”, the changes in the centroids of suitable habitats were calculated for three SSPs across two time periods (2041–2060 and 2081–2100) relative to the current centroid. An overall trend in distance changes was detected. The results indicated that the centroid of *T. mongolica* is in the northwestern part of Ordos. Under the SSP126 pathway, the distribution centroid exhibited a southeastward migration trend along the horizontal gradient. The SSP245 and SSP585 pathways showed northeastward and southeastward migration trends, respectively. Along the vertical gradient, *T. mongolica*

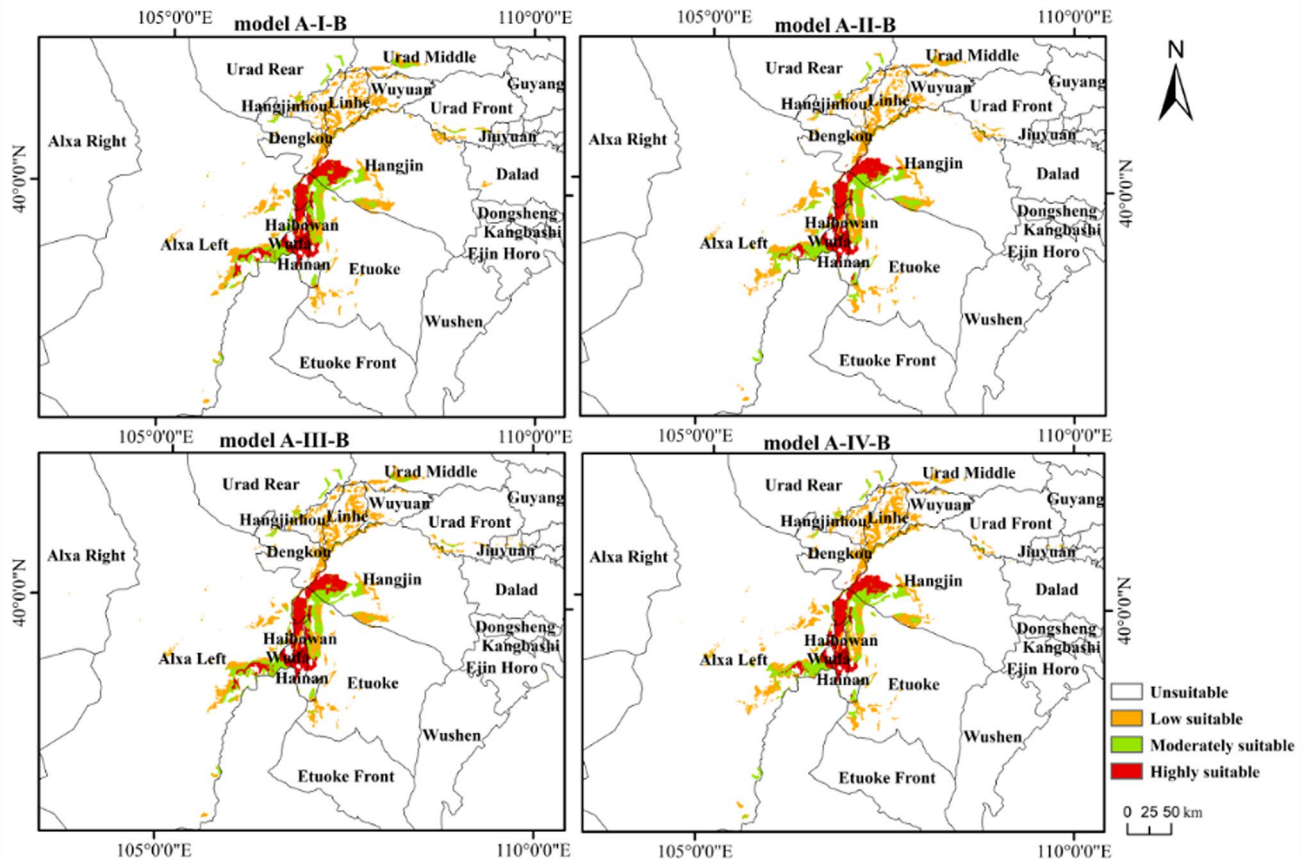


Fig. 6. Classification of dual habitat suitability distribution for *T. Mongolica* under current climate scenario. Maps created in ArcGIS 10.8 (<https://www.esri.com/zh-cn/arcgis/products/arcgis-desktop/resources>).

Model	Highly suitable habitat	Moderately suitable habitat	Low suitable habitat	Unsuitable habitat	Suitable habitat	Suitable habitat percent
Model A-I-B	0.2821	0.2951	0.5739	117.237	1.1511	0.9723%
Model A-II-B	0.2662	0.2881	0.5878	117.216	1.1421	0.9650%
Model A-III-B	0.2716	0.2768	0.5661	117.274	1.1145	0.9414%
Model A-IV-B	0.2575	0.2659	0.6078	117.226	1.1312	0.9558%

Table 1. The suitable habitat area of *T. mongolica* under current climate conditions is influenced by four different models ($\times 10^4$ km²).

migrated toward higher altitudes under the SSP126 pathway, whereas it initially migrated toward lower altitudes and then shifted to higher altitudes under the SSP245 and SSP585 pathways. However, the overall altitude change was insignificant and remained between 1,100 and 1,300 m (Fig. 9 and Table S5).

Discussion

This study utilized the MaxEnt model to generate Model A (climate niche model) and Model B (soil niche model), each with an AUC value > 0.9, indicating superior performance with high accuracy. Models A and B considered the effects of climate change scenarios and soil variables on *T. mongolica* distribution. Specifically, the four scenarios within Model A included climate, topography, NPP, and human activities, whereas Model B focused on soil texture and nutrient content. Constructing ENMs by considering multiple factors helps provide a comprehensive understanding of the potential ecological distribution patterns of *T. mongolica*. Recent studies have shown that soil and climate variables can be combined into a single niche model⁴³. Accordingly, the present study attempted this approach using climate and soil variables; however, the results indicated that the accuracy of the niche model did not improve significantly, and the model did not sufficiently account for soil impact (Table S1). The effectiveness of this method may be compromised by a correlation between soil and climate variables, potentially undermining their respective contributions to the model and prediction credibility⁴⁴ by treating soil variables as constants for future predictions⁴⁵. Therefore, the current study developed models A and B separately and integrated them using an “overlay function” to create a dual-suitability distribution of the

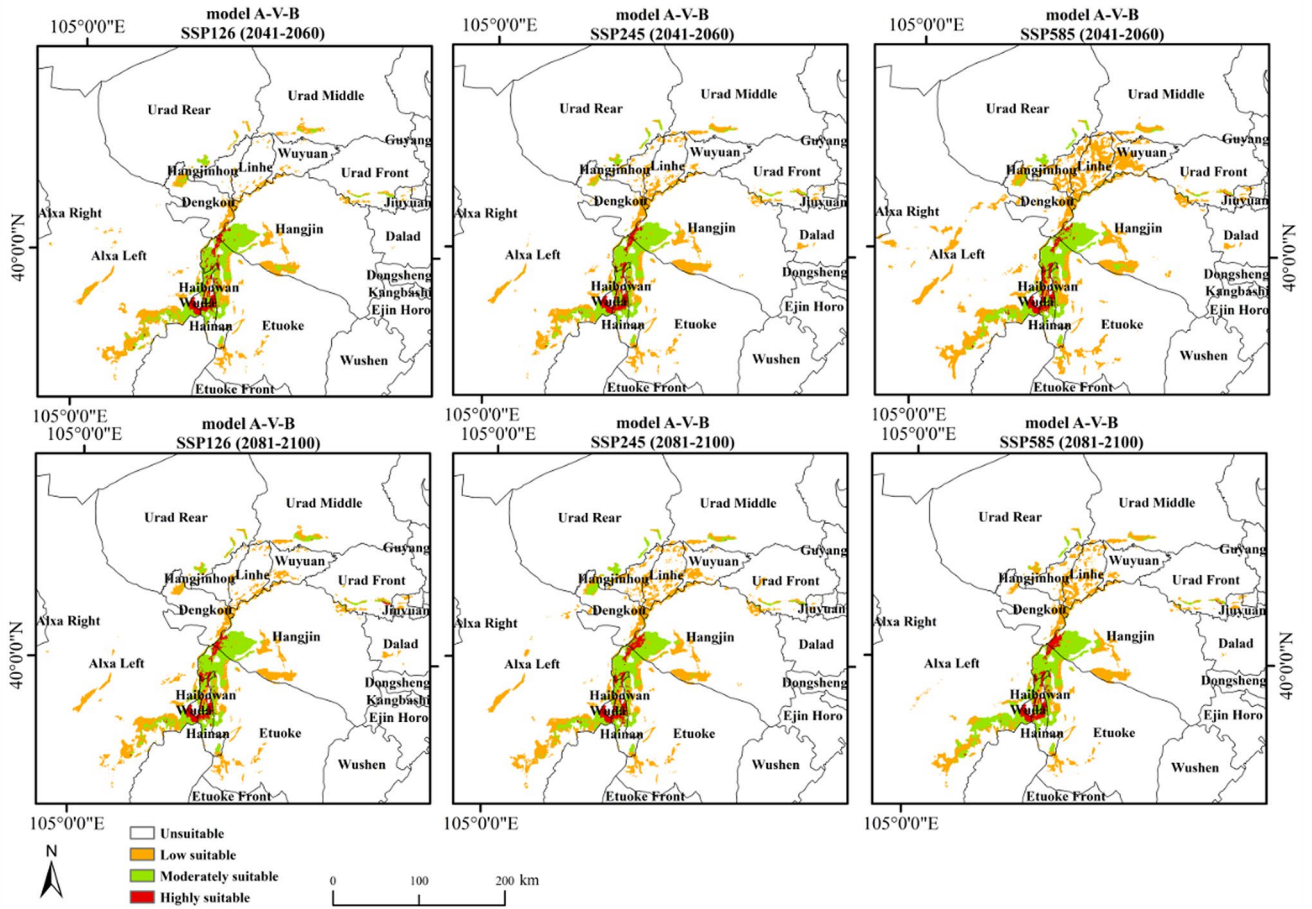


Fig. 7. Classification of dual habitat suitability projection for *T. mongolica* under future climate scenarios. Maps created in ArcGIS 10.8 (<https://www.esri.com/zh-cn/arcgis/products/arcgis-desktop/resources>).

Scenario	Time	Highly suitable habitat	Moderately suitable habitat	Low suitable habitat	Unsuitable habitat	Suitable habitat percent (%)
SSP126	2041–2060	0.0757	0.3801	0.5185	117.3256	0.8236
SSP245		0.0757	0.3678	0.5646	117.2919	0.8522
SSP585		0.0826	0.3944	0.9777	116.8453	1.2297
SSP126	2081–2100	0.0816	0.3531	0.5587	117.3067	0.8397
SSP245		0.0875	0.3642	0.6531	117.1953	0.9339
SSP585		0.0853	0.4076	0.5583	117.2489	0.8886

Table 2. The suitable habitat area for *T. mongolica* under future climatic conditions ($\times 10^4$ km²).

Scenario	Time	Highly suitable habitat			Moderately suitable habitat			Low suitable habitat		
		Gain	Loss	Unchanged	Gain	Loss	Unchanged	Gain	Loss	Unchanged
SSP126	2041–2060	0.0002	0.2355	0.08603	0.2453	0.1484	0.1879	0.2744	0.3375	0.3166
SSP245		0.0001	0.2366	0.0849	0.2375	0.1546	0.1817	0.2367	0.2473	0.4067
SSP585		0.0021	0.2294	0.0920	0.2512	0.1379	0.1983	0.5479	0.0876	0.5664
SSP126	2081–2100	0.0301	0.2315	0.0900	0.2308	0.1647	0.1716	0.2658	0.3710	0.2831
SSP245		0.0007	0.2225	0.0990	0.2400	0.1613	0.1750	0.2854	0.1952	0.4589
SSP585		0.0142	0.2257	0.0956	0.2585	0.2060	0.1303	0.2192	0.2370	0.4171

Table 3. The change in suitable habitat area of *T. mongolica* under future climatic conditions ($\times 10^4$ km²).

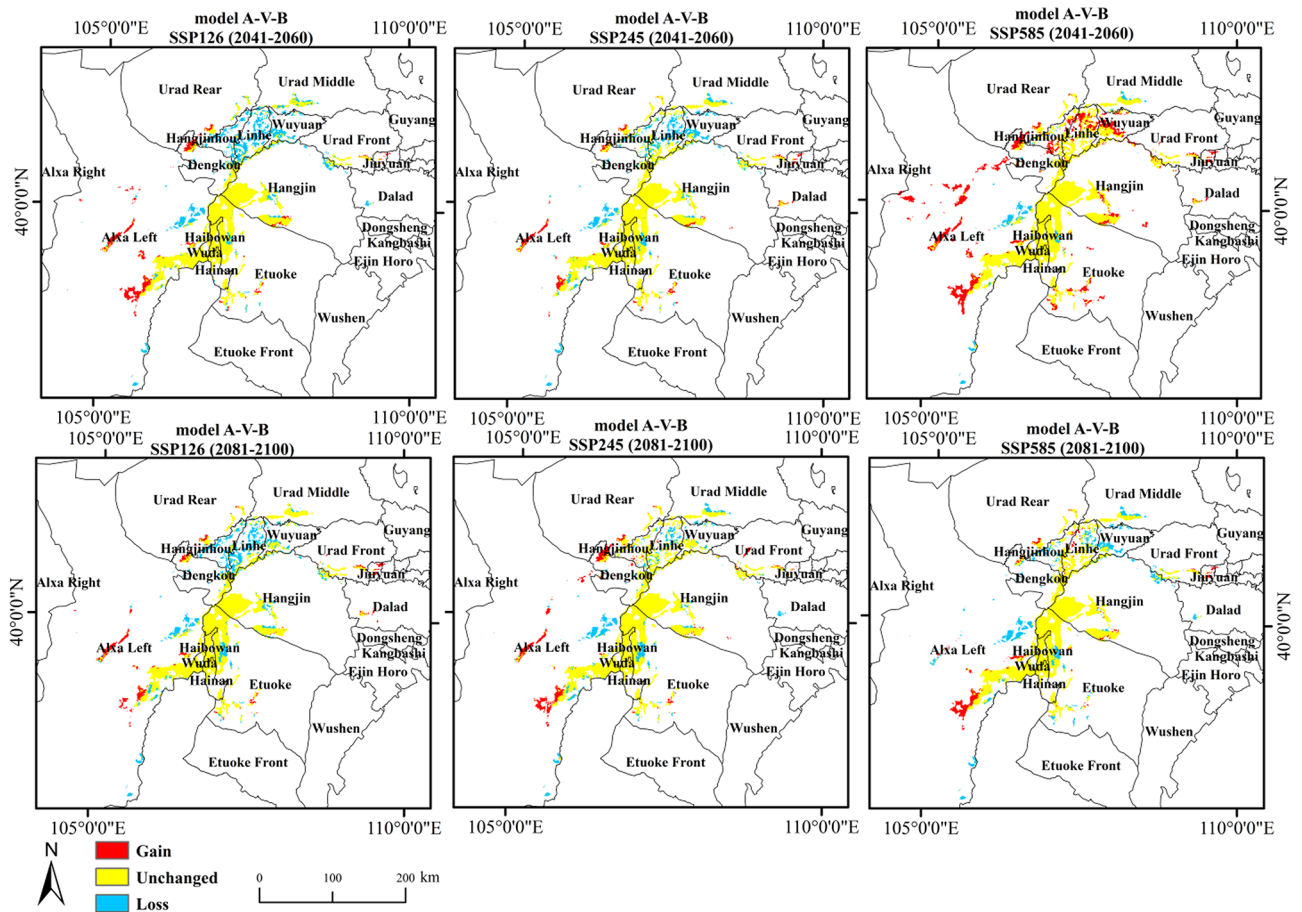


Fig. 8. Changes in the dual habitat suitability distribution for *T. mongolica* under future climate scenarios. Maps created in ArcGIS 10.8 (<https://www.esri.com/zh-cn/arcgis/products/arcgis-desktop/resources>).

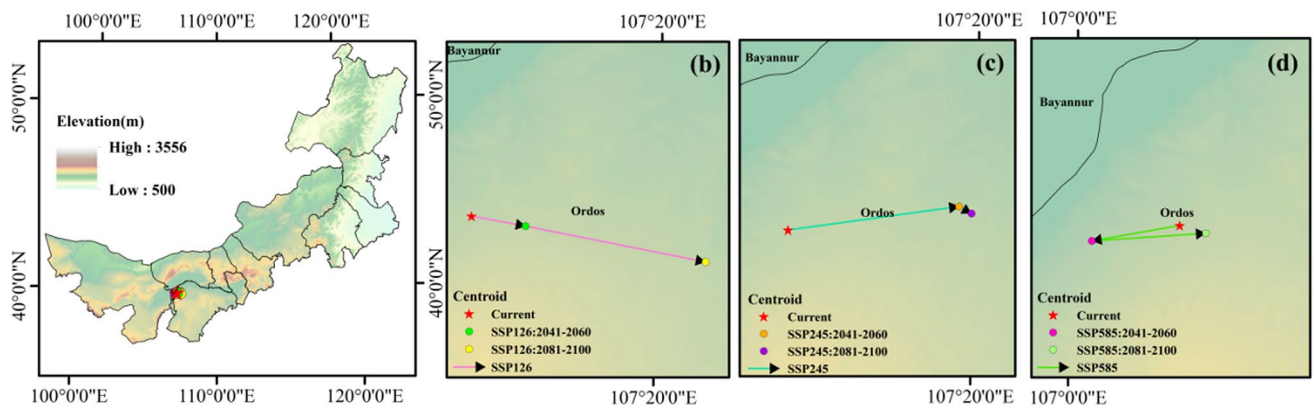


Fig. 9. Potential distribution centroid of *T. mongolica* under SSP126 (b), SSP245 (c), SSP585 (d). Maps created in ArcGIS 10.8 (<https://www.esri.com/zh-cn/arcgis/products/arcgis-desktop/resources>).

potential habitat of *T. mongolica*. The overlay process added constraints to prevent potential double counting or overlapping information. The minimum value between the two models was selected; when they were equal, the value from Model A was selected, ensuring the distribution of *T. mongolica*'s habitat met climate and soil suitability conditions. This approach maintains rationality by considering the combined impact of both factors on the distribution of *T. mongolica*'s habitat.

Identifying the key environmental variables determining species distribution is crucial for understanding the relationship between plants and their environment⁴⁵. *T. mongolica* thrives in desertified steppe regions characterized by a continental climate with high winds, abundant sand, drought, low rainfall, cold winters, hot

summers, and prolonged sunlight¹³. The ENM predicts that the primary variables influencing the potential geographic distribution of *T. mongolica* were climate change and human activities, specifically the minimum temperature of the coldest month (bio6), precipitation of the wettest month (bio13), precipitation of the driest month (bio14), and human activities. Incidentally, temperature and precipitation are the main factors affecting the growth of most plants⁴⁶. Temperature directly influences plant metabolic rate, and temperatures beyond the tolerance range can hinder plant growth and development⁴⁷. Prolonged elevated temperatures can disrupt internal physiological mechanisms and inhibit growth, whereas sustained low temperatures can cause frost damage or plant death⁴⁸. Precipitation directly affects soil moisture content, promoting a favorable plant growth environment. Adequate precipitation promotes growth and development, whereas insufficient rainfall can cause wilting and impede normal growth⁴⁹.

Human activities significantly influence species distribution by exerting inhibitory and promotional effects^{50,51}. Species such as *T. mongolica*, which have extremely limited distribution in China, play an essential role in local ecological conservation and ecosystem stability. Human activities such as mining, logging, grazing, land development, and urbanization have significantly reduced suitable habitats for *T. mongolica*. After incorporating human activities into the model (Model A-III-B), the overall suitable habitat area decreased by 3.1796% compared with that in Model A-I-B. Due to the simple community structure and fragile ecosystem of *T. mongolica*, human activities trigger habitat fragmentation²¹, resulting in distribution area reduction, a sharp decline in population numbers, and deterioration in the age structure, exacerbating the endangered status of the species. Therefore, human activities seriously threaten *T. mongolica*'s survival and reproduction, necessitating the strengthening of ecological conservation measures to mitigate further deterioration of its endangered status.

NPP determines the carbon sequestration capacity of ecosystems, directly affecting the absorption and release of carbon dioxide into the atmosphere. Hence, it is a vital indicator of ecosystem function and stability³⁰. Although the contribution of NPP to the models was not significant in models A-II-B and A-IV-B, the suitable habitat for *T. mongolica* decreased by 0.7819 and 1.7288%, respectively. This implies that NPP may indirectly influence plant distribution by affecting ecosystem structure and function⁵². While the direct contribution of NPP to *T. mongolica* distribution is limited, it may affect the distribution and growth of other vegetation types⁵³. A higher NPP may intensify competition among other vegetation types, indirectly affecting the suitable habitat of *T. mongolica*. Additionally, NPP reflects the ecosystem productivity level and health status, which are directly related to plant growth and distribution. Although the direct impact of NPP on *T. mongolica* distribution is limited, the influence of climate change on NPP may alter the health status of ecosystems⁵³, thereby affecting the suitable habitat of *T. mongolica*. Furthermore, when only NPP was considered, the contribution rate was low; however, a combined effect may occur when combined with human activities. These results suggest that compared with that in Model A-III-B, the suitable habitat area in Model A-IV-B increased by 1.4508%. This implies that including NPP may positively affect human activities, indirectly improving its impact on *T. mongolica* habitats by enhancing ecosystem productivity and function, thereby providing more suitable habitat conditions and areas for *T. mongolica*.

The soil niche model predicted that the topsoil sand fraction (T_SAND), soil unit symbol (SU_SYM90), topsoil sodicity (T_ESP), and topsoil gravel content (T_GRAVEL) significantly contribute to model predictions (Table S2). This suggests that areas where *T. mongolica* grows suffer from severe surface desertification and poor soil quality and are primarily characterized by desert and calcareous soils⁵⁴. In addition, the soil in these regions tends to be alkaline and contains a high proportion of gravel. Suitable soil conditions are crucial for *T. mongolica* growth. *T. mongolica* can increase the number of soil microbial species, alter their functionality, and enhance their diversity in the root zone. Therefore, when formulating conservation and planting strategies, climate factors should be considered the primary determining factors, while soil factors should be regarded as the limiting factors⁵⁵. For endangered relict species, areas where soil and climate conditions are suitable, known as double suitable areas, should be considered potential sites for planting and conservation. Further research on the growth of *T. mongolica* under varying climates and soil nutrient gradients will augment data on conservation planning.

For relict species such as *T. mongolica*, *Liriodendron chinense*, and *Liriodendron tulipifera*, suitable habitats are extremely limited and easily affected by climate change and topography, leading to reduction and even extinction⁶. This decline may be attributed to the lack of potential habitat areas for migration. Additionally, if only climatic factors are considered, the soils of some areas may not be suitable for *T. mongolica* growth, which could overestimate its suitable habitat. To provide more reliable predictions, we employed a dual-suitability approach to filter these areas (Fig. 4, Fig. S1). When considering soil factors, the predicted results showed a more pronounced reduction in suitable habitat areas (Fig. S1), consistent with previous findings⁵⁶. Therefore, predictive models that consider soil factors are more comprehensive and credible for guiding the conservation of relict species, including searching for new planting areas or high-quality seed sources⁵⁷.

Climate change poses unprecedented threats to biodiversity conservation and grassland ecosystem stability. Plant growth and distribution are profoundly affected by the increasingly evident impacts of climatic factors, such as rising temperatures and imbalanced precipitation. Therefore, the persistence of species depends on their ability to adapt to their habitat or migrate to cope with the uncertainty of future climate change⁵⁸. The predictive results of the present study indicate that the suitable habitat area for *T. mongolica* will decrease in the future (Figs. 7 and 8; Table 3) and may migrate toward the east (Fig. 9). With climate change, arid regions will become drier, especially in mid-to-high-latitude areas²⁵, exacerbating aridity in northwest China. Currently, *T. mongolica* is distributed in the arid regions of northwest China, mainly in the western parts of Inner Mongolia, and is concentrated in Wuhai and western Ordos (Fig. 8). Additionally, *T. mongolica* grows in rocky low mountains, gravel ridges, and piedmont alluvial fan areas at altitudes of 1000–1,300 m⁵⁹. Therefore, over time, the distribution center of *T. mongolica* may migrate eastward along the horizontal gradient, with minimal changes in the vertical gradient. Due to factors such as the soil environment, the migration distance of *T. mongolica* is limited.

Although this study incorporated soil factors to construct a dual-suitability model for *T. mongolica*, some limitations associated with data constraints are noted. First, the constructed ENMs considered soil factors but treated them as static. Currently, predicting future soil variables is not possible⁴⁴ due to their sensitivity to climate change and vegetation dynamics. This assumption might affect the accuracy of future predictions because changes in soil properties could significantly affect species distribution. Additionally, global warming may alter soil microbial activity distribution, affecting soil organic matter decomposition and thus influencing plant growth conditions⁶⁰. Therefore, existing models do not fully account for the dynamic changes in soil factors, potentially limiting the accurate prediction of future species distributions. Second, the future prediction results only considered the influence of climate change scenarios and did not fully consider other factors, such as human activities and NPP. This highlights the need for further research and model improvements to accurately predict future species distributions and consider the effects of multiple factors under future climate change.

Methods

Species occurrence data

T. mongolica data were obtained from the National Specimen Information Infrastructure (<http://www.nsii.org.cn/2017/home.php>), the Global Biodiversity Information Facility (<https://www.gbif.org/>, accessed on December 1, 2023), The Fourth Traditional Chinese Medicine Resources Survey of Inner Mongolia⁶¹, and published scientific literature¹². These sources yielded 4, 7, and 137 records of *T. mongolica*, respectively. To prevent information redundancy due to the spatial autocorrelation of sample points, the “Spatial Sparse Occurrence Data” tool in “SDMtoolbox” was used to filter the distribution data points of *T. mongolica* in the study area. Considering the elevation at which *T. mongolica* grows, we filtered 100 habitat distribution points for *T. mongolica* within a 1 km × 1 km grid area, ensuring no duplicate points existed (Fig. 10, Fig. S2).

Environmental variables

This study initially selected 42 environmental variables that could potentially influence *T. mongolica* distribution (Table S4). These included bioclimatic, soil, topographic, NPP, and human activity data. Nineteen bioclimatic variables were obtained from WorldClim version 2.1 (<https://www.worldclim.org>, released January 2020). Digital elevation model data were sourced from the Data Center for Resources and Environmental Sciences of the Chinese Academy of Sciences (<https://www.resdc.cn/>). Soil data were downloaded from the Harmonized World

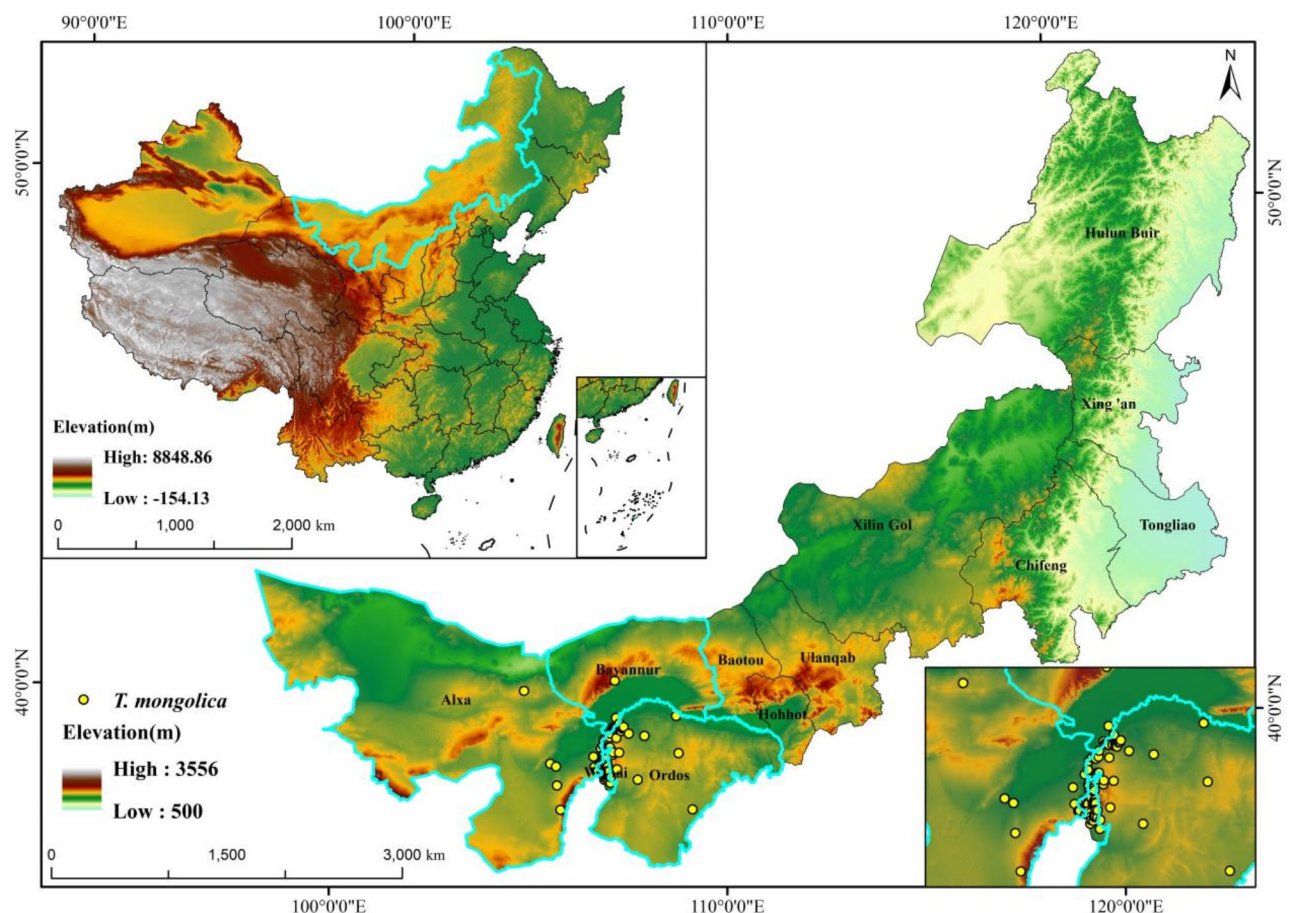


Fig. 10. Occurrence records of *T. mongolica* in Inner Mongolia, China. Maps created in ArcGIS 10.8 (<https://www.esri.com/zh-cn/arcgis/products/arcgis-desktop/resources>).

Soil Database version 1.2 (HWSD) (<http://www.iiasa.ac.at/>), which includes 30 soil parameters. These parameters are commonly used as soil indicators and are divided into topsoil (0–30 cm) and subsoil (30–100 cm) sections. These parameters include gravel content, silt fraction, sand, cation exchange capacity, which describes the soil's ability to retain and exchange cations; organic carbon, pH, and other ecologically significant physicochemical properties⁶². Since *T. mongolica* grows in environments with shallow and coarse soil layers⁶³, this study used 15 topsoil variables, 1 subsoil variable, and soil classification (SU_SYM90). These variables were extracted from the raster layers with a 30-arc-sec spatial resolution, and NPP data were obtained from the Chinese Science and Technology Resource Sharing Network (<https://escience.org.cn/>), which compiles monthly NPP data for terrestrial ecosystems in China north of 18°N latitude from 1985 to 2015⁶⁴, with a 1-km spatial resolution and units of gC/(m²a). These data objectively reflected the spatial variation in NPP in the grassland terrestrial ecosystems of Inner Mongolia, providing a reference indicator of the region's ecological environment. Human activity data were sourced from the Global Human Influence Dataset version 3 (https://www.ciesin.columbia.edu/wild_areas) and included annual records from 1993 to 2009 covering land use, population density, railways, roads, power infrastructure, croplands, and grazing⁶⁵. Weighted and standardized according to Sanderson et al., these data, with a spatial resolution of 1 km, objectively and comprehensively reflect the intensity and spatial distribution of human activities, demonstrating the degree of human environment disturbance in this study. All variables were resampled to a spatial resolution of 1 km using bilinear interpolation. We assumed that the topography and soil will remain largely under current and future conditions.

The climate data, including 19 bioclimatic variables, covered current and future conditions. Future climate data were based on the SSPs provided by the Intergovernmental Panel on Climate Change Sixth Assessment Report. The general circulation model selected for this study was BCC-CMS2-MR (China), which has shown improvements over the BCC-CMS1.1 m model in simulating global temperatures and the climatic distribution of annual precipitation in China⁶⁶. Given its appropriateness for China's climate change context, this model was selected to predict suitable habitats for *T. mongolica* in Inner Mongolia⁶⁷. Additionally, two time periods (2041–2060 and 2081–2100) and three climate change scenarios [SSP126 (optimistic: low-carbon emission pathway), SSP245 (moderate: medium-mitigation economic pathway), and SSP585 (pessimistic: high-emission economic pathway)] were selected.

Model construction

We constructed two models and five scenarios to investigate the influence of various factors on *T. mongolica*'s distribution (Table 4). The two models included the climate niche model (Model A) to simulate *T. mongolica*'s migration trends under different climate change scenarios and the soil niche model (Model B) to consider soil factor limitations on *T. mongolica*'s potential geographic distribution.

Model A comprised five scenarios: (I) Prediction of *T. mongolica* distribution under current climate change conditions, including environmental variables (bioclimatic + topographic); (II) Prediction of *T. mongolica* distribution under current climate change conditions, including environmental variables (bioclimatic + topographic) and NPP; (III) Prediction of *T. mongolica* distribution under current climate change conditions, including environmental variables (bioclimatic + topographic) and human activities; (IV) Prediction of *T. mongolica* distribution under current climate change conditions, including environmental variables (bioclimatic + topographic), NPP, and human activities; (V) Forecasting the distribution pattern of *T. mongolica* under future climate change scenarios, considering environmental variables (bioclimatic + topographic).

Scenarios I–IV were based on predictions under the current climate model, whereas V was based on a future climate model. Scenarios I–IV compare and analyze the impacts of climate, NPP, and human activities on the suitable habitats of *T. mongolica*, contrasting their effects under climate change.

Principal component analysis (Fig. S3) and Pearson's correlation analysis (Fig. S4) were performed while constructing the climate niche model to avoid model overfitting due to multicollinearity among the variables. Variables with a correlation coefficient (r) < 0.75 were selected to eliminate collinear and low-contribution variables, resulting in 12 representative variables used to construct of Model A⁶⁸. Seventeen soil variables were used to construct Model B (Table 5).

Construction and evaluation of the climate ecological niche model

To predict the potential distribution of *T. mongolica*, the climate ecological niche model employed the MaxEnt model (version 3.4.4) with default settings, following a conservative principle and replacing missing data with background points⁶⁹. Five hundred background points were randomly selected as pseudo-absences, with 75% of the occurrence records used for model training and 25% for testing. To reduce uncertainty, we conducted a 10-fold

Model	Scenario	Time	Variable				
			Climate	Topography	NPP	Human activities	Soil
Model A	I	Current	√	√	-	-	-
	II	Current	√	√	√	-	-
	III	Current	√	√	-	√	-
	IV	Current	√	√	√	√	-
	V	Future	√	√	-	-	-
Model B	-	Current & Future	-	-	-	-	√

Table 4. Model construction and variable selection.

Type	Variables	Description
Climate	bio3	Isothermally
	bio5	Max Temperature of Warmest Month
	bio6	Min Temperature of Coldest Month
	bio8	Mean Temperature of Wettest Quarter
	bio13	Precipitation of Wettest Month
	bio14	Precipitation of Driest Month
	bio15	Precipitation Seasonality
Topography	slope	Slope
	elevation	Elevation
	aspect	Aspect
Human activities	hf	Human Footprint
Ecology	NPP	Net Primary Productivity
Soil	T_GRAVEL	Topsoil Gravel Content
	T_SAND	Topsoil Sand Fraction
	T_SILT	Topsoil Silt Fraction
	T_CALY	Topsoil Clay Fraction
	T_USDA_TEX_CLASS	Topsoil USDA Texture Classification
	T_REF_BULK_DENSITY	Topsoil Reference Bulk Density
	T_OC	Topsoil Organic Carbon
	T_PH_H2O	Topsoil pH (H2O)
	T_CEC_CLAY	Topsoil CEC (clay)
	T_CEC_SOIL	Topsoil CEC (soil)
	T_BS	Topsoil Base Saturation
	T_TEB	Topsoil TEB
	T_CACO3	Topsoil Calcium Carbonate
	T_CASO4	Topsoil Gypsum
	T_ESP	Topsoil Sodicity (ESP)
	T_ECE	Topsoil Salinity (Elco)
	SU_SYM90	Soil Unit Symbol (FAO-90)

Table 5. Modeling variables.

cross-validation of the model, with an average of 10 repetitions considered the final result. Common evaluation metrics were used to quantify model performance, with the AUC of the receiver operating characteristic curve employed to assess accuracy. The AUC values were categorized as follows: 0–0.6 (Failed), 0.6–0.7 (Poor), 0.7–0.8 (General), 0.8–0.9 (Good), and 0.9–1.0 (Excellent)⁷⁰. Higher AUC values indicate better accuracy³⁹.

Construction of the soil ENMs

This study used HWSO data, which contains crucial soil information on the parameters that restrict *T. mongolica* distribution. However, among ENMs, only the MaxEnt model can accommodate categorical data as inputs for soil variables. Hence, we integrated 17 soil variables with *T. mongolica* occurrence data to establish Model B and determine the soil requirements for *T. mongolica* growth. To assess the performance of Model B, 75% of the occurrence data were used for model calibration and 25% for model validation. To enhance the credibility of the results, 10 repetitions were conducted, and model performance was evaluated using the AUC.

Integrating soil factors to predict the impact of climate change on *T. mongolica* distribution can be approached in two ways: combining climate and soil variables to build a model using traditional methods⁷¹, or separately establishing climate and soil ENMs⁷². Initially, we attempted to construct a combined model using 10 climatic and topographic variables and 17 soil variables. However, the performance of the combined model lacked significant improvement, and the importance ranking of the soil predictive factors remained low (Table S1), indicating that the model barely reflected the soil effects. Consequently, this study adopted the second approach. Following the “barrel effect” principle, the “overlay function” in ArcGIS was employed to perform layer stacking. Specifically, the *T. mongolica* climate suitability spatial distribution maps generated using Model A and the soil adaptability spatial distribution maps generated using Model B were overlaid. Climate suitability was the base, and the minimum value was retained⁷³. When the values were equal, those from Model A were selected (Fig. S1). Climate suitability and soil adaptability were integrated to obtain the dual suitability of *T. mongolica* for each grid, generating a spatial distribution map of dual suitability (Fig. S1), represented as Model A-I-B, Model A-II-B, Model A-III-B, Model A-IV-B, and Model A-V-B.

To analyze the changes in *T. mongolica*'s distribution patterns under different scenarios, this study employed the maximum training sensitivity plus specificity (MTSS) method to select the optimal threshold and binarize the predictive results for *T. mongolica*⁷⁴. Suitability was categorized into four groups: unsuitable (< MTSS), lowly

suitable habitat (MTSS=0.4), moderately suitable habitat (0.4–0.6), and highly suitable habitat (0.6–1) habitats⁴, using the same threshold for classification in current and future climate models.

Conclusion

Considering multiple factors, such as climate, soil, human activities, and topography, helps in understanding the effect of climate change on the potential distribution of *T. mongolica*. Climatic factors directly shape the growth environment of the plant, whereas soil conditions influence nutrient absorption and root growth, which are crucial for *T. mongolica*'s distribution. Human activities directly affect species habitat and growth conditions by altering vegetation cover and land use, while topographical factors shape growth environment and survival conditions^{75,76}. Although NPP may indirectly affect *T. mongolica*'s distribution, it still holds significance. It reflects plant growth rate and ecosystem productivity and indirectly influences the suitable habitat area and distribution pattern of *T. mongolica*. Despite its limited direct contribution to species distribution, NPP can indirectly ameliorate the impact of human activities on *T. mongolica* habitats by enhancing ecosystem productivity and functionality, thereby providing more suitable conditions for its survival. Therefore, comprehensive consideration of factors, such as climate, soil, human activities, topography, and NPP, is crucial for conserving and managing this species. By implementing more effective conservation and management measures, we can promote effective biodiversity protection and maintain the integrity and stability of ecosystems.

Data availability

All data generated or analysed during this study are included in this published article [and its supplementary information files].

Received: 1 October 2024; Accepted: 6 November 2024

Published online: 18 November 2024

References

- Zhang, M. et al. Influence of the Environment on the distribution and quality of *Gentiana Dahurica* Fisch. *Front. Plant. Sci.* **9**, 706822. <https://doi.org/10.3389/fpls.2021.706822> (2021).
- IPCC. *Climate Change 2014: Synthesis Report. Contribution of Working Groups I, II and III to the Fifth Assessment Report of the Intergovernmental Panel on Climate Change* (IPCC, 2014).
- Di Febbraro, M. et al. Different facets of the same niche: Integrating citizen science and scientific survey data to predict biological invasion risk under multiple global change drivers. *Glob Change Biol.* **29**, 5509–5523. <https://doi.org/10.1111/gcb.16901> (2023).
- Wang, D. et al. Moving north in China: the habitat of *Pedicularis kansuensis* in the context of climate change. *Sci. Total Environ.* **697**, 133979. <https://doi.org/10.1016/j.scitotenv.2019.133979> (2019).
- Morente-López, J. et al. Biogeographic origins and drivers of alien plant invasions in the Canary Islands. *J. Biogeogr.* **50**, 576–590. <https://doi.org/10.1111/jbi.14556> (2023).
- Shen, Y. et al. Predicting the impact of climate change on the distribution of two relict *Liriodendron* species by coupling the MaxEnt model and actual physiological indicators in relation to stress tolerance. *J. Environ. Manage.* **322**, 116024. <https://doi.org/10.1016/j.jenvman.2022.116024> (2022).
- Adhikari, D., Barik, S. K. & Upadhaya K. Habitat distribution modelling for reintroduction of *Ilex Khasiana* Purk., a critically endangered tree species of northeastern India. *Ecol. Eng.* **40**, 37–43. <https://doi.org/10.1016/j.ecoleng.2011.12.004> (2012).
- Rehan, M. et al. Application of species distribution models to estimate and manage the Asiatic black bear (*Ursus thibetanus*) habitat in the Hindu Kush Mountains, Pakistan. *Eur. J. Wildl. Res.* **70**, 1–11. <https://doi.org/10.1007/s10344-024-01806-2> (2024).
- Eyre, A. C. et al. Using species distribution models and decision tools to direct surveys and identify potential translocation sites for a critically endangered species. *Divers. Distrib.* **28**, 700–711. <https://doi.org/10.1111/ddi.13469> (2022).
- Niu, H. et al. Sustainable food systems under environmental footprints: The delicate balance from farm to table. *Sci. Total Environ.* **954**, 176761. <https://doi.org/10.1016/j.scitotenv.2024.176761> (2024).
- Guo, J. et al. Analysis of the distribution of *Astragalus membranaceus* var. *Mongolicus* in Inner Mongolia under climate change using the GEE platform. *Sci. Tradit. Chin. Med.* **2**, 237–244. <https://doi.org/10.1097/st9.0000000000000045> (2024).
- Yang, Y. et al. Comparative chloroplast genomics provides insights into the genealogical relationships of endangered *tetraena mongolica* and the chloroplast genome evolution of related Zygophyllaceae species. *Front. Genet.* **13**, 1026919. <https://doi.org/10.3389/fgene.2022.1026919> (2022).
- Cheng, J., Kao, H. & Dong, S. Population genetic structure and gene flow of rare and endangered *tetraena mongolica* Maxim. Revealed by reduced representation sequencing. *BMC Plant. Biol.* **20**. <https://doi.org/10.1186/s12870-020-02594-y> (2020).
- Dong, Z. Y. et al. Potential habitat prediction of *Tetraena mongolica* and its GAP analysis with nature reserves. *Arid Land. Geogr.* **46**, 595–603. <https://doi.org/10.12118/i.issn.1000-6060.2022.292> (2023).
- Zhen, J. et al. Climatic changes and its impact in the distributive region of *Tetraena mongolica* in the late 20th century. *J. Nat. Resour.* **24**, 1593–1603. <https://doi.org/10.11849/zrzyxb.2009.09.009> (2009).
- Duan, Y. Z. et al. Geographical distribution and prediction of potentially suitable regions of endangered relict plant *Tetraena Mongolica*. *Plant. Sci. J.* **37**, 337–347. <https://doi.org/10.11913/PSJ.2095-0837.2019.30337> (2019).
- Ruan, M., Zhang, Y. & Chai, T. Rhizosphere soil microbial properties on *Tetraena mongolica* in the arid and semi-arid regions, China. *Int. J. Environ. Res. Public Health.* **17**, 5142. <https://doi.org/10.3390/ijerph17145142> (2020).
- Xu, D. et al. High-throughput sequencing reveals the diversity and community structure in rhizosphere soils of three endangered plants in western ordos, China. *Curr. Microbiol.* **77**, 2713–2723. <https://doi.org/10.1007/s00284-020-02054-8> (2020).
- Henneron, L. et al. Rhizosphere control of soil nitrogen cycling: A key component of plant economic strategies. *New. Phytol.* **228**, 1269–1282. <https://doi.org/10.1111/nph.16760> (2020).
- Sugiyama, A. The soybean rhizosphere: Metabolites, microbes, and beyond—a review. *J. Adv. Res.* **19**, 67–73. <https://doi.org/10.1016/j.jare.2019.03.005> (2019).
- Liu, Z. et al. Fertile island' effects on the soil microbial community beneath the canopy of *Tetraena mongolica*, an endangered and dominant shrub in the West Ordos Desert, North China. *BMC Plant. Biol.* **24**, 178. <https://doi.org/10.1186/s12870-024-04873-4> (2024).
- Zhou, S. et al. Vegetation dynamics of coal mining city in an arid desert region of Northwest China from 2000 to 2019. *J. Arid Land.* **13**, 534–547. <https://doi.org/10.1007/s40333-021-0007-3> (2021).
- Wang, W. et al. Effect of coal mining activities on the environment of *Tetraena mongolica* in Wuhai, Inner Mongolia, China—a geochemical perspective. *Int. J. Coal Geol.* **132**, 94–102. <https://doi.org/10.1016/j.coal.2014.08.006> (2014).

24. Hu, Z. M. et al. Spatiotemporal dynamics of aboveground primary productivity along a precipitation gradient in Chinese temperate grassland. *Sci. China (Ser D- Earth Sci)*. **50**, 754–764. <https://doi.org/10.1007/s11430-007-0010-3> (2007).
25. Trenberth, K. E. Changes in precipitation with climate change. *Clim. Res.* **47**, 123–138. <https://doi.org/10.3354/cr00953> (2011).
26. Bardgett, R. D. et al. Combatting global grassland degradation. *Nat. Rev. Earth Environ.* **2**, 720–735. <https://doi.org/10.1038/s43017-021-00207-2> (2021).
27. Ni, J. Carbon storage in grasslands of China. *J. Arid Environ.* **50**, 205–218. <https://doi.org/10.1006/jare.2001.0902> (2002).
28. Mu, S. Assessing the impact of restoration-induced land conversion and management alternatives on net primary productivity in inner Mongolian grassland, China. *Glob Planet. Change*. **108**, 29–41. <https://doi.org/10.1016/j.gloplacha.2013.06.007> (2013).
29. Liu, L. et al. Characteristics of grassland degradation and driving forces in the source region of the Yellow River from 1985 to 2000. *J. Geogr. Sci.* **16**, 131–142. <https://doi.org/10.1007/s11442-006-0201-4> (2006).
30. Field, C. B. et al. Primary production of the biosphere: Integrating terrestrial and oceanic components. *Science*. **281**, 237–240. <https://doi.org/10.1126/science.281.5374.237> (1998).
31. Crabtree, R. et al. A modeling and spatio-temporal analysis framework for monitoring environmental change using NPP as an ecosystem indicator. *Remote Sens. Environ.* **113**, 1486–1496. <https://doi.org/10.1016/j.rse.2008.12.014> (2009).
32. Zhu, G. P. et al. Mapping the ecological dimensions and potential distributions of endangered relic shrubs in western Ordos biodiversity center. *Sci. Rep.* **6**, 26268. <https://doi.org/10.1038/srep26268> (2016).
33. Yang, M. et al. Ecological niche modeling of *Astragalus membranaceus* var. *Mongholicus* medicinal plants in Inner Mongolia, China. *Sci. Rep.* **10**, 12482. <https://doi.org/10.1038/s41598-020-69391-3> (2020).
34. Atwater, D. Z., Ervine, C. & Barney, J. N. Climatic niche shifts are common in introduced plants. *Nat. Ecol. Evol.* **2**, 34–43. <https://doi.org/10.1038/s41559-017-0396-z> (2018).
35. Guisan, A., Edwards, T. C. Jr. & Hastie, T. Generalized linear and generalized additive models in studies of species distributions: setting the scene. *Ecol. Model.* **157**, 89–100. [https://doi.org/10.1016/S0304-3800\(02\)00204-1](https://doi.org/10.1016/S0304-3800(02)00204-1) (2002).
36. Leathwick, J. R., Elith, J. & Hastie, T. Comparative performance of generalized additive models and multivariate adaptive regression splines for statistical modelling of species distributions. *Ecol. Model.* **199**, 188–196. <https://doi.org/10.1016/j.ecolmodel.2006.05.022> (2006).
37. Breiman, L. & Random Forests *Mach. Learn.* **45**, 5–32. <https://doi.org/10.1023/A:1010933404324> (2001).
38. Phillips, S. J., Anderson, R. P. & Schapire, R. E. Maximum entropy modeling of species geographic distributions. *Ecol. Model.* **190**, 231–259. <https://doi.org/10.1016/j.ecolmodel.2005.03.026> (2006).
39. Yang, W. et al. Dynamics of the distribution of invasive alien plants (Asteraceae) in China under climate change. *Sci. Total Environ.* **903**, 166260. <https://doi.org/10.1016/j.scitotenv.2023.166260> (2023).
40. Bosso, L. et al. Integrating citizen science and spatial ecology to inform management and conservation of the Italian seahorses. *Ecol. Inf.* **79**, 102402. <https://doi.org/10.1016/j.ecoinf.2023.102402> (2024).
41. Ahmadi, M. et al. MaxEnt brings comparable results when the input data are being completed; model parameterization of four species distribution models. *Ecol. Evol.* **13**, e9827. <https://doi.org/10.1002/ece3.9827> (2023).
42. Merow, C. & Silander, S. M. J. A practical guide to MaxEnt for modeling species' distributions: What it does, and why inputs and settings matter. *Ecography*. **36**, 1058–1069. <https://doi.org/10.1111/j.1600-0587.2013.07872.x> (2013). Jr.
43. Sehler, R. et al. Investigating relationship between soil moisture and precipitation globally using remote sensing observations. *J. Contemp. Water Res. Educ.* **168**, 106–118. <https://doi.org/10.1111/j.1936-704X.2019.03324.x> (2019).
44. Brun, P. et al. Model complexity affects species distribution projections under climate change. *J. Biogeogr.* **47**, 130–142. <https://doi.org/10.1111/jbi.13734> (2020).
45. Pecchi, M. et al. Species distribution modelling to support forest management. A literature review. *Ecol. Model.* **411**, 108817. <https://doi.org/10.1016/j.ecolmodel.2019.108817> (2019).
46. Jiang, H. et al. Determining the contributions of climate change and human activities to vegetation dynamics in agro-pastoral transitional zone of northern China from 2000 to 2015. *Sci. Total Environ.* **20**, 134871. <https://doi.org/10.1016/j.scitotenv.2019.134871> (2020).
47. Chang, Q. et al. Assessing variability of optimum air temperature for photosynthesis across site-years, sites and biomes and their effects on photosynthesis estimation. *Agric. Meteorol.* **298**, 108277. <https://doi.org/10.1016/j.agrformet.2020.108277> (2021).
48. Harsch, M. A. & HilleRisLambers, J. Climate warming and seasonal precipitation change interact to limit species distribution shifts across Western North America. *PLOS ONE*. **11**, e0159184. <https://doi.org/10.1371/journal.pone.0159184> (2016).
49. Xu, Z. et al. Effects of elevated CO₂, warming and precipitation change on plant growth, photosynthesis and peroxidation in dominant species from North China grassland. *Planta*. **239**, 421–435. <https://doi.org/10.1007/s00425-013-1987-9> (2014).
50. Amat, M. E., Vargas, P. & Gomez, J. M. Effects of human activity on the distribution and abundance of an endangered Mediterranean high-mountain plant (*Erysimum penyalarens*). *J. Nat. Conserv.* **21**, 262–271. <https://doi.org/10.1016/j.jnc.2013.02.001> (2013).
51. Yu, P. et al. Soil quality assessment under different land uses in an alpine grassland. *Catena*. **171**, 280–287. <https://doi.org/10.1016/j.catena.2018.07.021> (2018).
52. Cramer, W. et al. Comparing global models of terrestrial net primary productivity (NPP): overview and key results. *Global Change Biol.* **5**, 1–15. <https://doi.org/10.1046/j.1365-2486.1999.00009.x> (1999).
53. Chu, C. et al. Does climate directly influence NPP globally? *Global Change Biol.* **22**, 12–24. <https://doi.org/10.1111/gcb.13079> (2016).
54. Liu, J. et al. Effect of relict plant *Tetraena mongolica* on archaeal community in desert soil. *Acta Ecol. Sin.* **41**, 3548–3563. <https://doi.org/10.5846/stxb202003210634> (2021).
55. Muñoz-Rojas, M. et al. Climate and soil factors influencing seedling recruitment of plant species used for dryland restoration. *Soil*. **2**, 287–298. <https://doi.org/10.5194/soil-2-287-2016> (2016).
56. Arruda, D. M. et al. Combining climatic and soil properties better predicts covers of Brazilian biomes. *Sci. Nat.* **104**, 1–10. <https://doi.org/10.1007/s00114-017-1456-6> (2017).
57. Figueiredo, F. O. G. et al. Beyond climate control on species range: the importance of soil data to predict distribution of amazonian plant species. *J. Biogeogr.* **45**, 190–200. <https://doi.org/10.1111/jbi.13104> (2018).
58. Parmesan, C. & Yohe, G. A globally coherent fingerprint of climate change impacts across natural systems. *Nature*. **421**, 37–42. <https://doi.org/10.1038/nature01286> (2003).
59. Shi, S. L. et al. Variety of antioxidant system of *Tetraena mongolica* in different growth stages and habitats. *J. Desert Res.* **32**, 771–779 (2012).
60. Schindlbacher, A. et al. Temperature sensitivity of forest soil organic matter decomposition along two elevation gradients. *J. Geophys. Res. Biogeosci.* **115**. <https://doi.org/10.1029/2009JG001191> (2010).
61. Zhang, M. X. et al. Complex ecological and socioeconomic impacts on medicinal plant diversity. *Front. Pharmacol.* **13**, 979890. <https://doi.org/10.3389/fphar.2022.979890> (2022).
62. Wieder, W., Boehnert, J., Bonan, G. & Langseth, M. *Regridded Harmonized World Soil Database v12* (ORNL DAAC, 2014).
63. Liu, H. et al. Shifting plant species composition in response to climate change stabilizes grassland primary production. *Proc. Natl. Acad. Sci.* **115**, 4051–4056. <https://doi.org/10.1073/pnas.1700299115> (2018).
64. Chen, P. & Monthly, F. Dataset covering China's terrestrial ecosystems at North of 18°N (1985–2015). *J. Glob. Change Data Discovery*. **3**, 34–41. <https://doi.org/10.3974/geodp.2019.01.05> (2019).
65. Venter, O. et al. Global terrestrial human footprint maps for 1993 and 2009. *Sci. data*. **3**, 1–10. <https://doi.org/10.1038/sdata.2016.67> (2016).

66. Eyring, V. et al. Overview of the coupled model Intercomparison Project Phase 6 (CMIP6) experimental design and organization. *Geosci. Model. Dev.* <https://doi.org/10.5194/gmd-9-1937-2016> (2016). 9,1937–1958.
67. Yang, H., Jiang, Z. & Li, L. Biases and improvements in three dynamical downscaling climate simulations over China. *Clim. Dyn.* **47**, 3235–3251. <https://doi.org/10.1007/s00382-016-3023-9> (2016).
68. Liu, S. et al. Prediction of distributional patterns of four major *Camellia* oilseed species in China under climate and land use changes. *Ecol. Indic.* **155**, 110996. <https://doi.org/10.1016/j.ecolind.2023.110996> (2023).
69. Elith, J. et al. A statistical explanation of MaxEnt for ecologists. *Divers. Distrib.* **17**, 43–57. <https://doi.org/10.1111/j.1472-4642.2010.00725.x> (2011).
70. Swets, J. A. Measuring the accuracy of diagnostic systems. *Science*. **240**, 1285–1293. <https://doi.org/10.1126/science.3287615> (1988).
71. Xu, L. et al. Impacts of climate change and human activity on the potential distribution of *Aconitum Leucostomum* in China. *Sci. Total Environ.* **912**, 168829. <https://doi.org/10.1016/j.scitotenv.2023.168829> (2024).
72. Feng, L. et al. Predicting suitable habitats of *Camptotheca acuminata* considering both climatic and soil variables. *Forests*. **11**, 891. <https://doi.org/10.3390/f11080891> (2020).
73. Xu, W. et al. Assessment of the impact of climate change on endangered conifer tree species by considering climate and soil dual suitability and interspecific competition. *Sci. Total Environ.* **877**, 162722. <https://doi.org/10.1016/j.scitotenv.2023.162722> (2023).
74. Liu, C., Newell, G. & White, M. On the selection of thresholds for predicting species occurrence with presence-only data. *Ecol. Evol.* **6**, 337–348. <https://doi.org/10.1002/ece3.1878> (2016).
75. Buonincontri, M. P. et al. Shedding light on the effects of climate and anthropogenic pressures on the disappearance of *Fagus sylvatica* in the Italian lowlands: evidence from archaeo-anthracology and spatial analyses. *Sci. Total Environ.* **877**, 162893. <https://doi.org/10.1016/j.scitotenv.2023.162893> (2023).
76. Hussein, E. et al. (ed, A.) Do anthropogenic activities affect floristic diversity and vegetation structure more than natural soil properties in hyper-arid desert environments? *Diversity* **13** 157 <https://doi.org/10.3390/d13040157> (2021).

Acknowledgements

This study was supported by the China Agriculture Research System of MOF and MARA (Grant Nos. CARS-21), the Undergraduate Innovation and Entrepreneurship Training Program in Inner Mongolia Autonomous Region (Grant Nos. S202410130007).

Author contributions

All authors listed have made a substantial, direct, and intellectual contribution to the study. Conceptualization: J.G., M.Z., and Y.B.; Methodology: J.G.; Formal analysis: RW; Resources: J.G., M.Z., and Y.B.; Data curation: J.G.; Writing – original draft preparation: J.G., and Z.Z.; Writing – review and editing: J.G., and Z.Z.; Visualization: J.G.; Supervision: M.L.; Project administration: M.L. and J.G.; Validation: J.G., M.Z., Z.Z. and Y.B.; Funding acquisition: M.L. All authors have read and agreed to the published version of the manuscript.

Declarations

Competing interests

The authors declare no competing interests.

Additional information

Supplementary Information The online version contains supplementary material available at <https://doi.org/10.1038/s41598-024-79088-6>.

Correspondence and requests for materials should be addressed to M.L.

Reprints and permissions information is available at www.nature.com/reprints.

Publisher's note Springer Nature remains neutral with regard to jurisdictional claims in published maps and institutional affiliations.

Open Access This article is licensed under a Creative Commons Attribution-NonCommercial-NoDerivatives 4.0 International License, which permits any non-commercial use, sharing, distribution and reproduction in any medium or format, as long as you give appropriate credit to the original author(s) and the source, provide a link to the Creative Commons licence, and indicate if you modified the licensed material. You do not have permission under this licence to share adapted material derived from this article or parts of it. The images or other third party material in this article are included in the article's Creative Commons licence, unless indicated otherwise in a credit line to the material. If material is not included in the article's Creative Commons licence and your intended use is not permitted by statutory regulation or exceeds the permitted use, you will need to obtain permission directly from the copyright holder. To view a copy of this licence, visit <http://creativecommons.org/licenses/by-nc-nd/4.0/>.

© The Author(s) 2024